Report series ISSN 0284-2769 of

THE SVEDBERG LABORATORY and
DEPARTMENT OF RADIATION SCIENCES
UPPSALA UNIVERSITY

Box 535, S-75121 Uppsala, Sweden

http://www.tsl.uu.se/

TSL/ISV-2005-0291

March 2005

A method for measuring light ion reaction cross sections

R.F. Carlson[1],* A. Ingemarsson[2,3],† M. Lantz[2],‡ G.J. Arendse[4], A. Auce[2], A.J. Cox[1], S.V. Förtsch[5], M.N. Jacobs[4], R. Johansson[2], J. Nyberg[2], J. Peavy[1], P.-U. Renberg[3], O. Sundberg[3], J.A. Stander[4], G.F. Steyn[5], G. Tibell[2], and R. Zorro[6]

[1] Department of Physics, University of Redlands, Redlands, CA. 92373, U.S.A.

[2] Department of Radiation Sciences, Box 535, S-75121 Uppsala, Sweden

[3] The Svedberg Laboratory, Box 533, S-75121 Uppsala, Sweden

[4] Department of Physics, University of Stellenbosch, Private Bag X1, Matieland 7602, South Africa

[5] iThemba Laboratory for Accelerator-Based Sciences, Faure, South Africa

[6] Department of Engineering Sciences, Uppsala University, Box 534, S-75121 Uppsala, Sweden

An experimental procedure for measuring reaction cross sections of light ions in the energy range 20-50 MeV/nucleon, using a modified attenuation technique, is described. The detection method incorporates a forward detector that simultaneously measures the reaction cross sections for five different sizes of the solid angles in steps from 99.1 to 99.8% of the total solid angle. The final reaction cross section values are obtained by extrapolation to the full solid angle.

PACS numbers: 25.40.Ep 25.45.De 25.55.Ci 24.10.Ht 29.40.Mc 29.27.Eg

I. INTRODUCTION

The optical model has been very succesful in reproducing angular distributions of elastic scattering of nucleons and ions from nuclei. However, the fact that different optical potentials may predict the same angular distributions, but different reaction cross section values, reveals the need for directly measured reaction cross sections, σ_R. The experimental efforts in the past have mainly focused on measuring angular distributions for as many targets and energies as possible, while relatively few measurements of the complementary reaction cross section have been performed.

The reaction cross section gives the probability that a particle will undergo a nonelastic process when undergoing a nuclear interaction. The reaction cross section is the sum of all nonelastic nucleon-nucleus interaction cross sections, including secondary particle production. Reaction cross section data are of importance, not only from a theoretical point of view but also for a variety of research fields and technical applications. There are several applications in medicine, for instance in radiation therapy, patient dosimetry, and radioisotope production, where the cross sections for protons, neutrons and light ions are important. In astrophysics the formation and evolution of stars, and certain properties of neutron stars, can be better understood if reliable cross sections are available. The recent interest in Accelerator Driven Systems (ADS) for energy production and transmutation of long lived nuclear waste requires better knowledge of the reactions occuring when an intermediate energy proton beam induces an intense flow of neutrons and other reaction products in a thick high-Z target through the spallation process. The OECD Nuclear Energy Agency (NEA) has issued a report on an evaluation of nucler data needs for applications at intermediate energies [1]. The report includes a High-Prioriy Nuclear Data Request List (HPRL), and proton reaction cross sections are required for 8 out of the 10 selected nuclei in the HPRL.

A collaboration was established between groups at Uppsala University and the University of Redlands with the purpose of measuring reaction cross sections of light composite particles on various nuclei in the energy region 20-50 MeV per nucleon. The experimental technique, originally used by the Redlands group for measurements of proton reaction cross sections in

*Electronic address: Richard_Carlson@redlands.edu
†Electronic address: Anders.Ingemarsson@tsl.uu.se
‡Electronic address: Mattias.Lantz@tsl.uu.se

the energy region 20-50 MeV, was based on a variation of a standard attenuation method, and has been described in an earlier report [2].

Initially the same experimental technique was used as that for the earlier proton measurements. Events were excluded from analysis if any particle entered a region in the forward direction that subtended a cone of about 0.6% of the total solid angle. The missing solid angle was corrected for under the assumption that the flux of reaction products inside the cone was not more than twice as large as the average flux outside the cone. This correction would then have a negligible effect on the error associated with these measurements.

In the first measurement at Uppsala, for α-particles [3], large discrepancies were observed between the experimental reaction cross sections and optical model calculations. Therefore, in the subsequent measurement for deuterons [4], three different sizes of the unanalyzed forward region were used in order to investigate the influence of the size of this region on the final σ_R value. It was discovered that the measured reaction cross sections exhibited a strong sensitivity to the size of the excluded forward cone, and that this effect was energy dependent.

Therefore the experimental technique was modified so that results could be obtained simultaneously for several different sizes of the excluded forward cone. We will here denote these values as *partial reaction cross sections*. The measurement for α-particles was repeated [5] with much better agreement with the theoretical predictions. Recently reaction cross sections for ^{3}He were measured [6], and these data, together with the earlier data for α-particles and deuterons, should lead to a better understanding of the microscopic features of reaction cross sections. A measurement has also been performed with 65 MeV protons [7], and further measurements at higher proton energies are presently being conducted in collaboration with groups from the University of Stellenbosch and the iThemba Laboratory for Accelerator-Based Sciences.

The purpose of this report is to describe the modified experimental procedure and the methods for data extraction that were utilised. The following section gives an overview of the principles of measurement. In section III the transmission method is described, followed by the developments during the Uppsala measurements in section IV. A detailed description of the experimental apparatus is given in section V, and section VI describes the data analysis.

II. PRINCIPLES OF MEASUREMENT

When a beam of nuclear particles is incident on a thin target, particles may either pass through the target without any interaction, be elastically scattered, or interact nonelastically with the target. The reaction cross section, σ_R, is defined as the probability that a projectile will undergo any nonelastic interaction with the target, and can be determined from

$$I_u + I_{el} = I_0 \cdot exp(-nx\sigma_R), \tag{1}$$

where I_0 is the number of incident particles, I_u is the number of particles that have passed the target without any interaction, I_{el} is the number of elastically scattered particles, and nx is the number of target nuclei per unit area. For thin targets, where $nx\sigma_R \ll 1$, the expression may be expanded and written in the form

$$\sigma_R = \frac{I_0 - I_u - I_{el}}{nxI_0}, \qquad \text{or} \qquad \sigma_R = \frac{I_0 - I}{nxI_0}. \tag{2}$$

The difference $I_0 - I_u - I_{el}$ is the number of nonelastic interactions that occurs. The projectile can be removed from the elastic scattering channel through different processes, and the reaction cross section is the sum of all nonelastic cross sections. Usually $I_u + I_{el}$ is denoted I, but the distinction between the unaffected beam and the elastically scattered particles is made because in the present experiment the unaffected beam is handled differently than the particles that have been scattered by a measurable angle.

For a target with known thickness, nx, an experimental determination of the reaction cross section requires a measurement of the three quantities I_0, I_u and I_{el}. Due to the infinite range of the Coulomb potential there is no clear boundary between unaffected beam particles and those that are elastically scattered in the forward direction. Although the principle of measurement is very simple it turns out to be difficult in practice, and has resulted in relatively few reaction cross section measurements.

In an earlier report by the Redlands group [2] a brief review of different experimental methods that had been used up to that time was given. Since then a number of measurements have been performed with a variety of projectiles, a few of them with new experimental approaches.

The method of using the energy dependence of the attenuation in a detector as a means of measuring the reaction cross section, earlier limited exclusively to detector materials, has

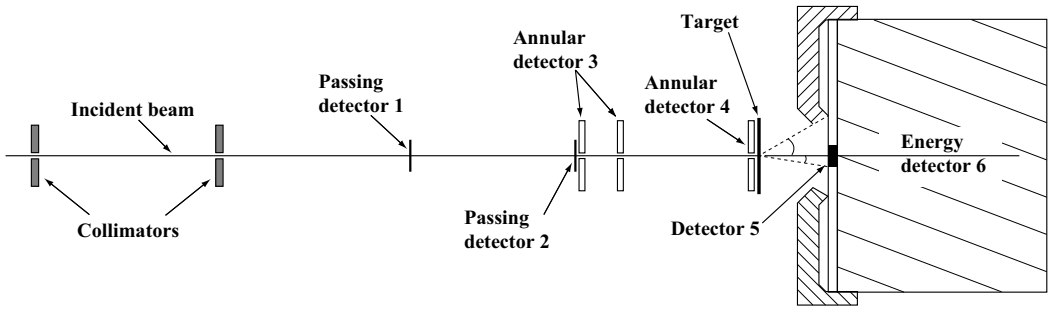

FIG. 1: Schematic diagram of the reaction cross section apparatus.

been extended by Warner *et al.* [8] to include other target materials by using several layers of detectors interlayered by thin sheets of the target material.

Mittig *et al.* [9] have used a 4π detector array to measure the associated γ-rays from reactions. This method works well under the assumption that each nuclear reaction is followed by the emission of at least one γ-ray.

An inexpensive but laborious method is to determine the reaction cross section with solid state nuclear track detectors [10], where the target surface is etched after irradiation, followed by visual identification of nuclear reactions in the target material itself.

The method described in this report is a modification of the attenuation technique that was described in [2].

III. THE TRANSMISSION METHOD

The basic idea of the transmission method is to count all particles incident on the target as well as all unaffected and elastically scattered particles in the forward direction. An experimental arrangement, shown in Fig. 1, usually consists of three main parts. First the incident particles are identified in a transmission telescope to ensure a geometrically well defined beam. The second part is the target system where a thin target is positioned. Finally there are detectors to distinguish reaction products from non-reaction and elastically scattered particles, usually by an energy measurement of the ejectiles. By performing a series of target-in and target-out measurements contributions not due to the target can be eliminated.

The identification of non-reaction particles can be made with a total absorption (energy)

detector. The main problem with such a detector is that it cannot distinguish between reactions that have occurred in the target and reactions occuring in the detector itself. Usually the target thickness is small in comparison with the stopping range of the projectiles. Therefore most of the particles detected with an energy below the elastic peak are those that have undergone reactions in the detector itself. Thus the number of reactions can only be obtained by subtracting two large and nearly equal numbers of nonelastic events from the target-in and target-out measurements. This requires considerable beam time in order to obtain statistically accurate values. A thicker target improves the situation, but due to the increased energy loss in the target this also increases the uncertainty of the energy at which the reaction cross section is measured.

An important improvement to the method was introduced in the 1960's and was based on the observation that due to the nature of the Coulomb scattering most of the non-reaction particles, 98% or more, are concentrated in a narrow forward cone, while the reaction products and nonelastic particles are more or less isotropically distributed.

A forward cone of about 10° angle covers less than 1% of the total solid angle. If the distribution of reaction products is fairly isotropic the number of reaction products entering the forward cone will be small. Thus particles that enter the narrow forward cone are excluded from the analysis. If the effect of the excluded forward cone is corrected for by an extrapolation to the full solid angle, it should have a small effect on the measured reaction cross section. The exclusion of the forward cone significantly improves the statistical accuracy because the number of false reaction events is reduced, and the difference between the target-in and target-out measurements is mainly due to true reaction events.

The narrow forward cone behind the target is defined by a small transmission detector (detector 5 in Fig. 1) which is centered with respect to the beam and placed immediately in front of the energy detector 6. This detector produces a veto pulse in the electronics if hit by any particle. The rejection of particles in the forward cone works well under the assumption that the reaction products, with the exception of low lying states, are isotropically distributed. But the method is not applicable if the reaction products are strongly forward peaked so that more than 2-3% of them are inside the forward cone. This was found to be the case for the measurements of light composite particles at Uppsala and led to further development of the method.

IV. THE UPPSALA EXPERIMENTAL PROGRAM

A. Initial measurements

Almost all reaction cross section measurements before the Uppsala measurements were performed by excluding the forward cone under the assumption of an isotropic distribution of the reaction products, after corrections for low lying states within the resolution of the energy detector. The missing reaction events within the excluded forward cone then could be corrected for by assuming that the missing reaction cross section was proportional to the solid angle of the excluded forward cone.

The measurements were performed with an apparatus originally designed and used by the Redlands group for measurements of proton reaction cross sections in the energy region 20-50 MeV [2]. The intention of the Uppsala-Redlands effort (begun in 1992) was to measure reaction cross sections for light composite particles in the energy region 20-50 MeV per nucleon, and it was assumed that the same approach could be used as in the earlier proton measurements.

This assumption was supported by the fact that although many direct reactions are forward peaked, their contribution to the reaction cross section is relatively small, and the scattering into the continuum is expected to be isotropically distributed. Furthermore, with the very small solid angle of the excluded forward cone the effects of the non-isotropy on the results were expected to be a negligible fraction of the measured reaction cross section.

The disagreement between the measured reaction cross sections for α-particles [3] and optical model predictions [11] led to the conclusion that there was a significant systematic error in the measurements. This indicated that a modification of the experimental strategy would be required.

B. The modified technique

As a result a measurement of reaction cross sections for deuterons was performed with three different sizes of the forward cone detector 5 [4]. From this measurement it became evident that there was a considerable flux of reaction products in the forward direction and that this flux increased with increasing energy. The difference in reaction cross sections measured with the different excluded forward cones was significant and was not consistent

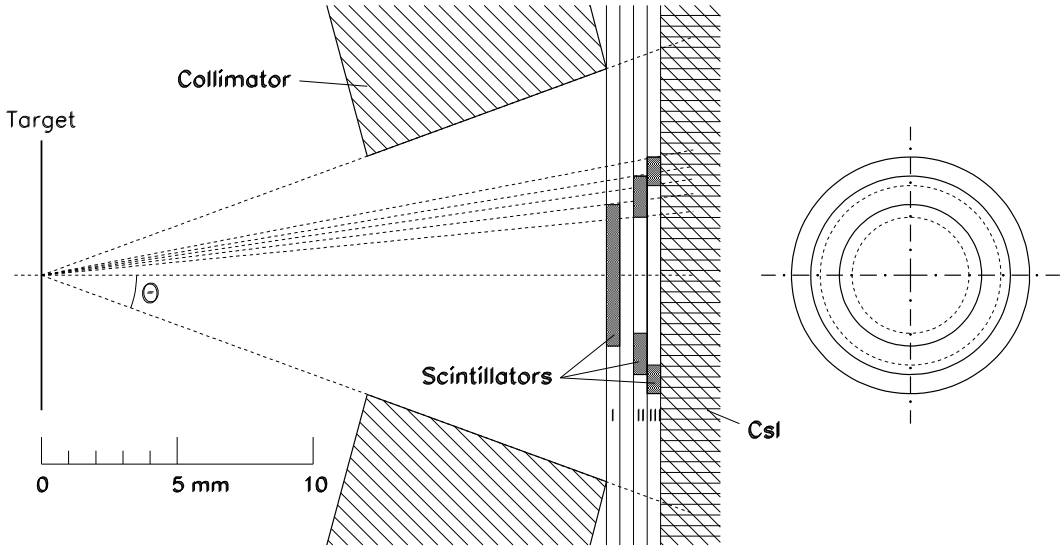

FIG. 2: Details of the target, the angle defining collimator and detectors 5 and 6. The circular scintillator is followed by two ring scintillators, the overlap creates 5 forward cones. The CsI energy detector is directly behind the last ring scintillator. The righthand figure shows the three scintillators, as seen in the beam direction.

with the assumption of an isotropic distribution of the reaction products.

After the deuteron experiment detector 5 was replaced with an array of three overlapping veto detectors covering five different solid angles, as shown in Fig. 2. Through this arrangement five forward cones are defined, making it possible to simultaneously measure the reaction cross section outside of each excluded forward cone (partial reaction cross sections), covering five different solid angles between 99.1% and 99.8% of the total solid angle. With this arrangement the measured partial reaction cross sections were used with an extrapolation to obtain the reaction cross section for the full solid angle. This new detector array was used to repeat the α-particle measurement [5].

Since the range and hence the light output per MeV for composite particles such as ^{3}He and ^{4}He is considerably smaller than that for protons and deuterons, the light output from two breakup products can be larger than for elastically scattered ^{3}He or ^{4}He particles. For this reason the energy (stopping) detector was chosen to be thick enough to just totally absorb elastically scattered projectile particles (^{3}He or ^{4}He). In this way the possibility that both breakup products could be stopped in the detector was eliminated.

V. EXPERIMENTAL DETAILS

A. Particle beams

The experiments have been performed at the The Svedberg Laboratory (TSL), Uppsala, with particle beams from the Gustaf Werner Cyclotron. All internal parts of the experimental apparatus described below are held at vacuum with a pressure of approximately 10^{-3} mbar or less.

Due to the use of a CsI stopping detector, which has a slow signal compared with plastic scintillators, the experiment requires a beam with very low intensity, of the order of 10^4 particles per second. This is obtained by reducing the intensity in the ion source in combination with several attenuating collimators along the beamline between the cyclotron and the experimental setup.

The alignment of the beam and the apparatus is crucial for these measurements. The two collimators in Fig. 1 both have 1 mm holes and are separated by 5 meters. The size of the transmitted beam with these collimators is so small that only slit-scattered particles will hit outside the central region of detector 5. In order to minimize the slit-scattering, the alignment of the beam was performed with two pairs of steering magnets, coupled to each other in such a way that the position of the beam could be changed without any change of the direction and vice versa. The advantage with this method is that it eliminates the sensitivity to the alignment of the beam phase ellipse. In the second step of the alignment the apparatus was adjusted vertically and horisontally with an accuracy within 0.01 degrees. It also turned out that the slit-scattering was sensitive to the focusing of the beam and the best conditions were obtained when the beam was convergent between the two collimators.

B. Identification of particles

The presence of a particle in the incident beam is made known by signals produced in a passing detector telescope (see Fig. 1) containing two passing detectors and two annular detectors. The first two detectors, denoted passing detectors 1 and 2, each consist of a rectangular plastic scintillator (NE102 sheet) of thickness 0.076 mm and 6 mm sides. The scintillators are viewed by RCA8575 photomultipliers.

After passing detector 2 there are two active collimators, the annular detectors 3 and 4.

Detector 3 consists of a pair of plastic scintillator discs, made of 1.1 mm thick NE102A. The first disc is 3 mm from the second passing detector and has a hole of 2.30 mm diameter located at its centre, while the second disc has a hole of 3.05 mm diameter. These are mounted in a polished lucite holder which is covered with aluminised mylar. The holder acts as light guide, and the entire assembly slides into a cavity in the apparatus. The scintillator discs are held perpendicular to the beam, while the centre holes are concentric with the beam. The two discs are positioned at 2.5 cm distance from each other, and the second disc is 19.2 cm from the target. Each viewing cavity is vacuum sealed with a lucite disc, and both ends of the assembly are viewed by RCA8575 photomultipliers. Detector 4 is identical to detector 3, except that it contains only one disc, with a centre hole of 2.30 mm diameter. The disc is positioned 4.9 cm from the target.

The output signals from detectors 3 and 4 are in anti-coincidence with the coincidence output from detectors 1 and 2. If a beam particle is scattered in the forward direction by any of the passing detectors, or from the collimator edges, it will enter detector 3 and/or 4 and be rejected. Only particles passing through the holes of the annulars detectors satisfying $12(\overline{3+4})$ will be counted as trigger events that reach the target; the number of trigger events is denoted I_0.

C. Targets

The targets, all solid and in the mass range from ^{9}Be to ^{208}Pb, are composed of thin circular foils, approximately 1.2 cm in diameter, and are considerably larger than the diameter of the beam. The targets have areal densities of about 50 mg/cm^2, resulting in beam energy losses of a few MeV.

Accurate determination of target areal density and thickness uniformity is crucial for an accurate measurement of the reaction cross section. In order to determine the average areal density each target is weighted on an electronic balance which is accurate to $\pm$0.01 mg. Its diameter is measured to an accuracy of $\pm$0.005 cm. This results in a 1% uncertainty in the average areal density. The thickness non-uniformity varies from 0.1% to 4%, depending on the target material, and is determined by the target manufacturer.

The target foils are mounted in a wheel which accomodates 13 different targets and 2 empty spaces for target-out measurements. A stepping motor, remotely operated from the

control room, turns the wheel to the position of the next target, indicated by a potentiometer connected to the wheel axis. This allows the targets to be positioned in the beam to an accuracy of about 0.5 mm.

D. Angle defining collimator

Immediately following the target is a brass collimator which defines the maximum angle for scattering into detector 6. The collimator angle is between 20° and 30° and is optimised for each energy; a small angle gives large uncertainties in the elastic scattering corrections while a large angle reduces the energy resolution in detector 6 due to recoil effects.

E. Detector 5

The set of three plastic detectors now comprising detector 5 is shown in Fig. 2. The scintillators are of type BC400 and are 0.5 mm thick. They are embedded in 0.5 mm thick plexiglass plates that act as light guides. Each light guide passes out through slots on either side of the target block assembly and is viewed by two RCA8575 photomultipliers placed on opposite sides. Each light guide plate is covered with 0.02 mm thick aluminised mylar in order to avoid light leakage from one light guide to another. The first scintillator (5_I) is a circular disc with a diameter of 5.24 mm, while the second (5_{II}) and third (5_{III}) are annular rings with inner and outer diameters of 4.30 and 7.35 mm and 6.65 and 8.77 mm, respectively. Table I gives all details of the scintillator geometries. The overlap between the scintillators defines five different forward angular regions, and makes it possible to simultaneously measure the partial reaction cross sections for five different effective sizes of detector 5 (denoted Ω_j in Table I). From these cross section values an extrapolation to the full solid angle can be made (see section VI B 1). The number of counts in each region also gives information on the differential cross section for the elastic as well as the total nonelastic scattering.

TABLE I: Effective forward cones, Ω_j, and angular regions defined by logical combinations of the three detectors 5_I, 5_{II} and 5_{III} shown in Fig. 2. θ_{max} gives the maximum scattering angle for each region, r the maximum radius of the detector and d the distance to the target. The solid angles outside the forward cones are also given in per-cent of the total solid angle. The last column gives the logical combination used to define the forward cones and the angular regions.

	θ_{max}	r	d	Solid angle	Analyzed	Logical
	°	(mm)	(mm)	(msr)	region(%)	combination
Ω_1	5.622	2.150	21.84	30.226	99.760	$5_I\overline{5_{II}}$
Ω_2	7.179	2.620	20.80	49.261	99.608	5_I
Ω_3	8.451	3.325	22.38	68.217	99.457	$(5_I+5_{II})\overline{5_{III}}$
Ω_4	9.552	3.675	21.84	87.107	99.307	(5_I+5_{II})
Ω_5	11.087	4.385	22.38	117.267	99.067	$(5_I+5_{II}+5_{III})$
Region 0	5.622	2.150	21.84	30.226		$5_I\overline{5_{II}}$
Region 1	7.179	2.620	20.80	18.956		5_I5_{II}
Region 2	8.451	3.325	22.38	19.001		$\overline{5_I}5_{II}\overline{5_{III}}$
Region 3	9.552	3.675	21.84	18.890		$\overline{5_I}5_{II}5_{III}$
Region 4	11.087	4.385	22.38	30.160		$\overline{5_I5_{II}}5_{III}$

F. Energy detector

Directly behind detector 5 is the energy analyzing detector 6, which is composed of a CsI(Na) scintillator with a specific thickness for each energy. CsI has a much lower ionization quenching effect than plastic scintillators. This, in combination with a thickness that just stops elastically scattered particles, reduces the probability that two or more breakup fragments, or other reaction products, give pulse heights greater than those from elastically scattered beam particles.

The back of the CsI scintillator is attached to a 3 mm thick glass light guide, connected to an RCA8575 photomultiplier. The energy resolution of detector 6 is 1.5-2 MeV FWHM for the regions covered by detector 5, and 2.5-4 MeV in the region outside of detector 5.

G. Electronics and data acquisition system

A schematic drawing of the electronics is shown in Fig. 3. The detector signals are sent to a distant counting room, where they are processed with standard NIM electronics. All detector signals, except for the CsI, are sent to the electronics directly from the photomultipliers without any amplification. The signals from the detectors with two photomultipliers are gain-matched to each other and summed with T-connectors.

Signals are sent to a scaler for online monitoring of beam intensity and detector performance. The rest of the electronics is activated when there are signals from the passing detectors 1 and 2 in coincidence. This trigger opens the gates on the ADC, QDC (charge-integrating ADC), pattern unit and event trigger unit, and signals are recorded from each detector channel. The fast signals from the plastic scintillators are processed by the QDC, while the slower CsI signal goes through a shaping amplifier before being processed by the ADC. An event trigger unit sends a veto signal to the coincidence unit during the time the data acquisition system is busy with conversion and readout. Pileup rejection signals from passing detector 2 and the CsI are registered by a pattern unit. This feature, which is needed due to the long recovery time of the CsI, excludes events in which two consecutive particles from different beam micropulses go through the passing detector telescope within 15 μs of each other. A Time-to-Amplitude-Converter (TAC) starts on the coincidence signal and stops on the signal from the first pileup unit, giving information on the time structure of the beam, and enables further pileup vetoing. From the QDC, ADC, pattern unit and scaler the signals are sent to the data acquisition system.

Data are recorded event by event, using the MIDAS [12] based general purpose data acquisition system SVEDAQ at TSL [13]. Data are read out through a CAMAC branch highway and sent to a VME-based event builder. From the event builder system, data are split into two independent branches, one to an Exabyte tape station for recording, and the second one to online analysis. A SUN workstation is used for online sorting, monitoring and control. Typical online spectra that can be displayed are pulse heights from the detectors, timing characteristics and beam intensity.

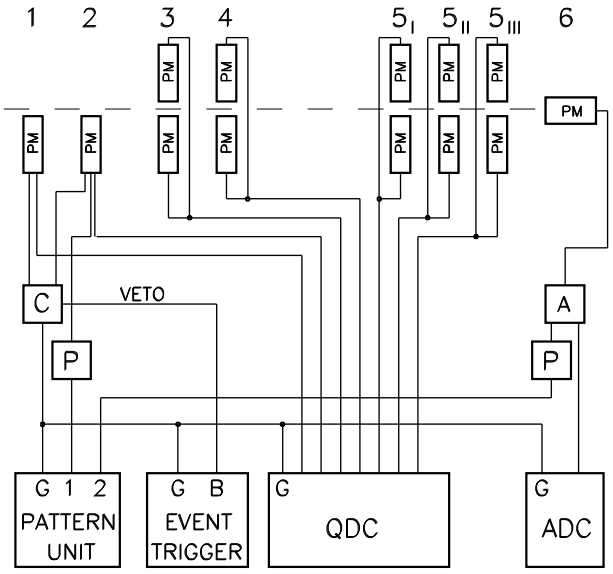

FIG. 3: Schematic drawing of the electronics setup. A signal from the coincidence unit (C) opens the gates (G) on the ADC, QDC, pattern unit and event trigger when there are signals in coincidence from 1 and 2. Pileup events are registered by the pattern unit when pileup units (P) detect two events within 15 μs of each other from either detector 2 or from the amplified (A) signal from detector 6.

VI. DATA COLLECTION AND ANALYSIS

A series of 2 to 4 target-in/target-out measurements, each consisting of about $5{\cdot}10^6$ incident beam particles, are performed. Each measurement takes typically 15-30 minutes.

A. Analysis and corrections to the raw data

After the experiment the recorded data are sorted with an analysis program written in Fortran 77. Discriminator levels for each detector can be set in the program. In the program a trigger event is defined from the double coincidence-anti coincidence requirement on the signals from detectors 1-4 in the passing detector telescope, $I_0 = 12(\overline{3+4})$, thereby selecting only properly directed beam particles. An additional constraint for I_0 is that the pattern unit has not registered any pileup signal from the detector system. Thus the full definition of a trigger event means that a beam particle was correctly directed onto the target, and was neither preceeded nor followed by another beam particle within 15 μs. From the identified

trigger events a non-attenuation event, I, is defined if the unaffected beam particle deposits energy in detector 6 within the discriminator levels for the elastic peak. These numbers have to be corrected for the limited detection efficiency in the CsI detector, as discussed below in section VI A 2.

For a given set of discriminator levels the program obtains I_0 and I for each forward region 1-5, and the corresponding i_0 and i from target-out measurements. Fig. 4 shows typical energy spectra for target-in and target-out measurements in each forward region. The measured background is very small in all regions except for region 1. As shown in the figure the elastic events can fairly easily be distinguished from the attenuation events (reaction events) in each region, and this improves the accuracy of the analysis compared to setting one discriminator level for all regions of detector 6. Region 5 covers a larger angular region than the other regions and due to the larger variation in recoil and energy loss the energy resolution is not as good as for the other regions. The number of elastic events in each region is corrected for the limited detector efficiency in detector 6 (see section VI A 2). Thereafter the uncorrected partial reaction cross section, σ_{un}, is obtained for each excluded forward cone according to the logic conditions in Table I. Then the weighted mean from different runs is calculated for each target and for the runs without target, followed by other corrections. In the following paragraphs the corrections applied to the partial reaction cross sections are described.

1. Elastic scattering

Elastically scattered particles emerging at angles greater than the one given by the angle defining collimator will not be registered in detector 6. These nonreaction events are falsely counted as reaction events since there is no signal in detector 6. This is corrected for by subtracting the elastic differential cross sections, integrated between the collimator angle and 180°, from the experimentally measured σ_{un}. The corrections are calculated from global optical potentials or taken from published data on elastic cross sections or optical potentials. Due to the forward peaking of elastic scattering these corrections can be limited to a few percent. If no data are available at the given energy, or for a given target isotope, then interpolations from available data of other energies or isotopes are performed, resulting in larger uncertainties to the corrections.

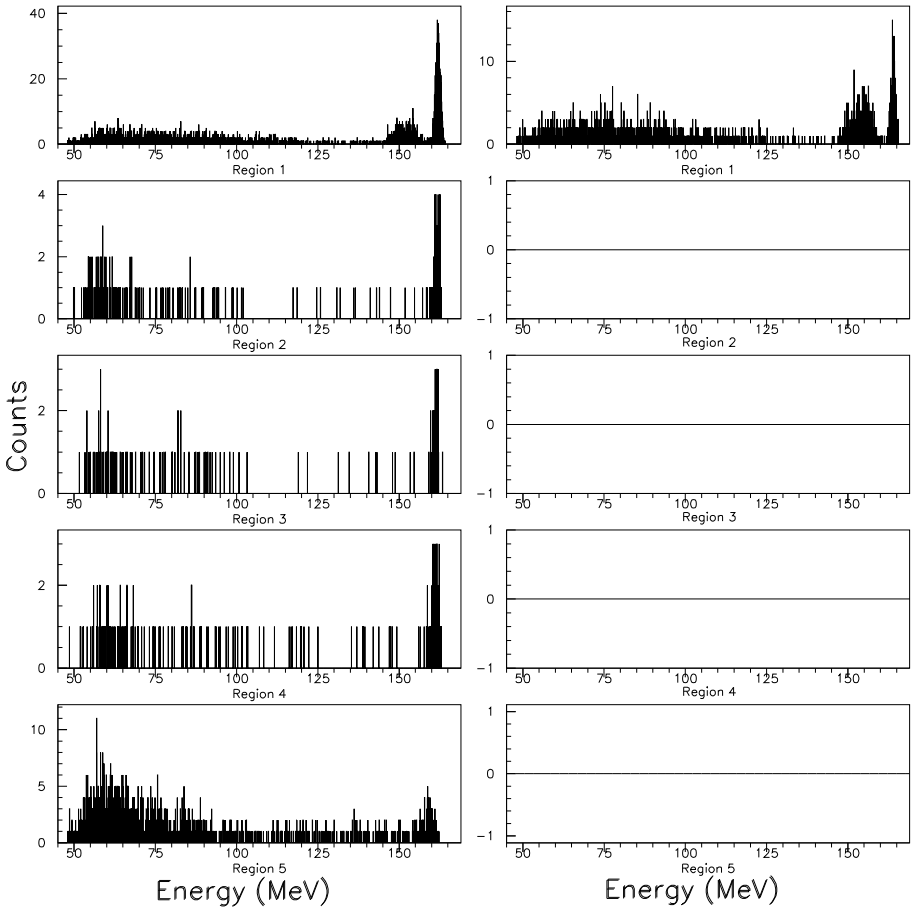

FIG. 4: Energy spectra of regions 1-5 obtained for 167 MeV ^{3}He-particles with the target ^{40}Ca (left) and without target (right).

2. Reactions in detector materials

Some particles, elastically scattered or unaffected by the target, lose energy through nuclear reactions in the material of detector 6. This results in signals corresponding to energies below the elastic peak, and thus produces false reaction events. Since more than 99.9% of the particles are unaffected by the target, the detector efficiency can be determined and corrected for in each run by counting all elastic events that are registered in region 0 and comparing this number with the total number of events in region 0, assuming that all of them are elastic events. The detector efficiency is energy dependent and might therefore differ for target-in and target-out measurements, but due to the thin targets used the difference is negligible. For instance in the ^{3}He measurement the detector efficiency was 98.1% at 96 MeV and 95.9% at 167 MeV, and the detector efficiencies for target-in and target-out differed by

less than 0.1% at each energy. The detector efficiency also depends on the incident particle type, but for all measurements the corrections were of the order of a few percent. The error introduced by this correction, due to the fact that a few of the events in region 0 are true reaction events in the target, is negligible. The measured detector efficiency also includes reactions that occur in the scintillators or light guides of detector 5.

3. Other corrections

Corrections due to finite target thickness and finite beam size have been estimated to be negligible.

B. Evaluation of data

For each run, with or without target, the analysis of the data and the inclusion of the corrections discussed above proceeded in the following way. With the aid of the signals from the scintillators and the E-detector it was possible to follow each particle through the detector system. From the particles in region 0 the detection efficiency for the E-detector was derived. In the next step the first partial reaction cross section was obtained from the number of particles which had given a trigger but no signal from detectors 5 and 6. This partial reaction cross section thus gives the number of reactions, when all events producing one particle inside the opening angle of the collimator, approximately 30°, are excluded from the analysis. This number should of course be corrected for elastically scattered particles outside the collimator, as described in section 6.1.1, but this correction can also be made at a later stage since it is the same for all partial reaction cross sections. Thereafter the number of reaction events for particles with a signal in detector 6 but no signal in detector 5 was added. This number of reactions obtained from the energy spectrum of region 5 (see Fig.4) has to be corrected for the limited detection efficiency of elastic scattering and is calculated from the number of elastic events and the detection efficiency. This correction leads to a decrease of the number of reactions and an increase of the associated error, which is rather small outside region 1. In this way the first partial reaction cross section shown in the figures 5 and 6 was obtained. It gives the number of reactions when all particles hitting detector 5 are excluded from the analysis. After this the same procedure was repeated for

regions 4, 3, 2 and 1 to obtain all partial reaction cross sections. For each step the values obtained without target were subtracted from those with target.

1. Extrapolation procedure

When all the corrections above are completed one obtains the partial reaction cross sections for five solid angles, each excluding a forward cone Ω_j, where j is 1-5, see Table I. The partial reaction cross sections are given by

$$\sigma_{R_j} = \frac{1}{nx}\left[\frac{(I_0 - I)}{I_0} - \frac{(i_0 - i)}{i_0}\right] - \Delta\sigma_{el}, \tag{3}$$

where $\Delta\sigma_{el}$ is the correction for elastic scattering outside the detector. The corrections for reactions in detector materials have been included in the terms $I_0 - I$ and $i_0 - i$.

The final result for the reaction cross section is obtained through extrapolation of the partial reaction cross sections to the full solid angle. We have performed measurements with three projectiles: protons, ^{3}He and ^{4}He. We also have some information from our earlier measurement for deuterons, but this information is less complete, as explained below, since these measurements of different partial reaction cross sections were not performed simultaneously.

For the measurements with protons at 65 MeV the extrapolation resulted in an increase of the reaction cross section of 1-2%, when extrapolating from 8.9°. In the measurements for protons in the energy region 80 to 180 MeV (preliminary results presented at the ND2004 conference [16]) it was found that this correction first slightly increased to 3-4% and then was almost constant. At no energy the partial cross sections indicated a deviation from a linear dependence on the excluded solid angle. The extrapolation was therefore performed with straight lines, as illustrated in Fig. 5 for 180 MeV protons from ^{12}C. The errors were obtained from a χ^2-fitting procedure.

For deuterons the extrapolation from 8.9°, which corresponds to 99.4% of the solid angle, increased the partial reaction cross section with 2.0%, 4.9% and 12.4% at 37.9, 65.5 and 97.4 MeV, respectively. Also for deuterons straight lines were used for the extrapolation.

For ^{3}He and ^{4}He the extrapolation curves are remarkably similar as a function of energy per nucleon and the effects are much larger. We also observed a systematic deviation from a linear dependence on the excluded solid angle. For this reason the extrapolation was

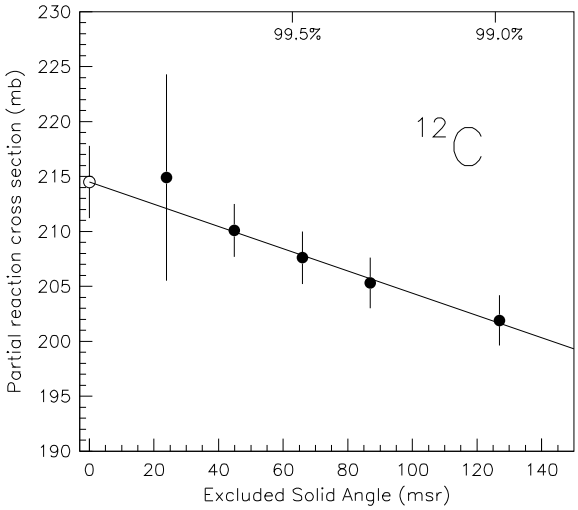

FIG. 5: The partial reaction cross sections for 180 MeV proton on ^{12}C and the extrapolation to the full solid angle. The extrapolated value is shown by the open circle.

performed with second order polynomials. The same method was used by Renberg *et al.* [14] for reaction cross sections for protons in the energy region 220-570 MeV. Figs. 6 and 7 in Ref. [14] show that the partial reaction cross sections for protons vary almost linearly with the excluded solid angle at 234 MeV, whereas the results at 554 MeV are very similar to those we have for ^{3}He and ^{4}He. A non-linear dependence was also observed by Dietrich *et al.* [15] with 1380 MeV protons. Renberg *et al.* [14] also performed the extrapolation assuming that the differential cross section for the total inelastic scattering is given by

$$\left(\frac{d\sigma}{d\Omega}\right)_{inel} = Ae^{-B\theta^2}, \tag{4}$$

where θ is the scattering angle and A and B constants. This method , however, gave almost exactly the same result. Fig. 6 shows the corrected partial reaction cross sections for 192.4 MeV α-particles on ^{12}C, plotted versus the solid angle for each excluded forward cone. The errors were also in this case estimated from a χ^2-fitting procedure. As seen, the open circle which shows the extracted value, has considerably larger errors than most of the partial reaction cross sections.

In summary, we have observed a large flux of particles in the forward direction of the order of several b/sr for ^{3}He and ^{4}He. If we had performed one single measurement covering 99.8% of the total solid angle we should have no information at all on the flux into the excluded forward cone. Furthermore, an extrapolation to the full solid angle, assuming

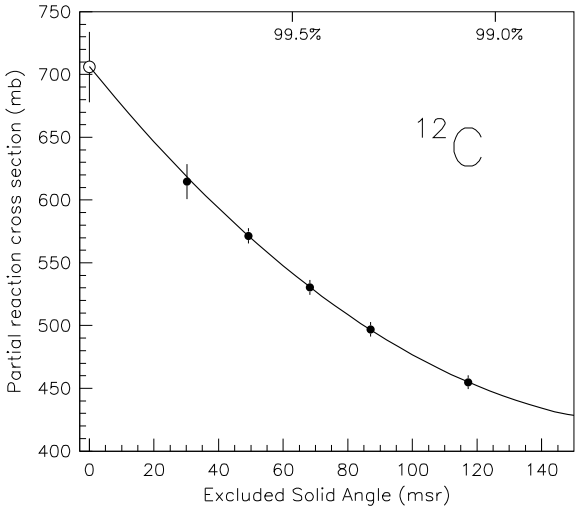

FIG. 6: The partial reaction cross sections for 192.4 MeV α-particles proton from ^{12}C and the extrapolation to the full solid angle. The extrapolated value is shown by the open circle.

an isotropic distribution of the reaction products, should have resulted in a serious error also for protons. It should be stressed that to cover more than 99.8% of the total solid angle is almost impossible, due to slit-scattering in the collimators and Coulomb scattering in the passing detectors. The fact that several partial reaction cross sections are measured simultaneously is also crucial. If the partial reaction cross sections are measured individually, the contributions from the inner regions will be obtained from the difference between large numbers with large statistical errors. Therefore simultaneous measurements of several partial reaction cross sections give much more detailed information on details important for the extrapolation procedure.

Normally all direct interactions are considered to be forward peaked, but in this case we consider angles up to 10°. Since strong collective quadrupole and octupole excitations have their maxima outside our forward cone, they will only give small contributions to the forward peaking. Also angular distributions for breakup, which have their maximum at 0°, will predominantly contribute to the reaction cross section outside the forward cone if one takes into account the solid angle. The effects we have observed indicate that the angular distribution of the total inelastic scattering is similar to those of monopole transitions.

The size of the effects we have observed indicates that it must be reactions in the continuum which contribute to the forward peaking. As discussed by Chang [17] the continuum shape looks quite different for (α, α') than for (^{6}Li,^{6}Li') and (^{12}C,^{12}C'). The large probability

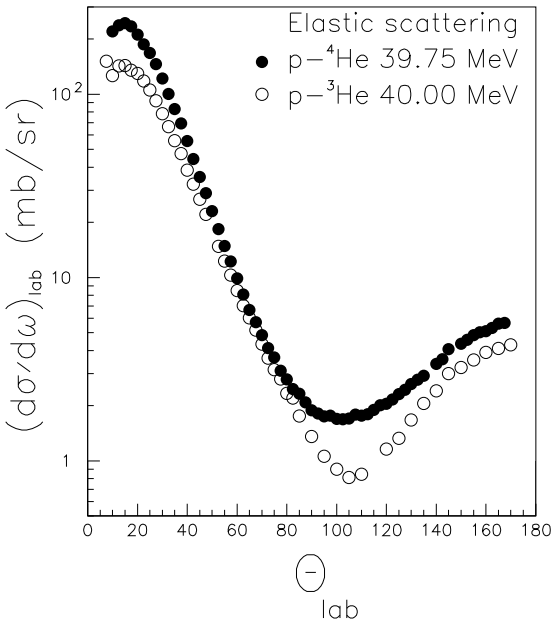

FIG. 7: Angular distributions of the differential cross sections for proton scattering from ^{3}He at 40 MeV and from ^{4}He at 39.75 MeV.

for large energy losses in inelastic α-scattering should thus not be due to collective excitations. Proton scattering from ^{3}He and ^{4}He has shown that for both of these targets there is a large probability for backscattering. This is illustrated in Fig. 7 which shows the angular distributions of the differential cross sections in the scattering of protons from ^{3}He at 40 MeV [18] and from ^{4}He [19] at 39.75 MeV. It should be noted that in the backscattering of a heavy projectile from a light target, both are scattered at very small angles in the laboratory system.

One possibility to explain the strong forward peaking for ^{3}He and ^{4}He could thus be to suppose that ^{3}He and ^{4}He are backscattered from individual nucleons in the target. Such an assumption is supported by the fact that in backscattering of these ions there is a very large tranfer of momentum, which should make the projectiles sensitive to nucleon dimensions in the nucleus.

Finally we want to state that reaction cross section measurements for charged particles are very complicated due to the large flux of reaction products at very small angles. The flux differs drastically for different projectiles and we see no possibility to predict the flux

for a specific projectile. Whereas we had expected the largest flux for the loosely bound deuteron we observed the largest flux for the extremely stable ^{4}He.

2. Uncertainties in the final result

The statistical uncertainties in $I_0 - I$ and $i_0 - i$ are the major sources of error in the experiment, while the uncertainties in the correction terms, except for the elastic scattering correction, are negligible. The total statistical uncertainty is of the order of 5%. The uncertainties in target thickness and thickness uniformity are presented separately and are of the order of a few percent.

VII. FURTHER MODIFICATIONS OF THE EXPERIMENTAL SETUP

After the last experiment at the TSL [6] the experimental setup was transferred to the iThemba Laboratory for Accelerator-Based Sciences (Faure, South Africa), and further modified in order to accommodate measurements of protons with beams from the iThemba Separated Sector Cyclotron in the energy range 80-180 MeV. The major changes of the experimental setup are of geometrical nature and involve thicker targets, thicker collimators, new scintillator dimensions in detector 5, and a large CsI energy detector which absorbs protons up to 200 MeV. Electronics and data acquisition systems differ in details, but the measurement principles and analysis methods are basically the same as the ones used in the Uppsala experiments and described earlier in this report.

VIII. CONCLUSIONS

The attenuation method previously used for 20-50 MeV protons [2] has been modified for measurements of reaction cross sections of deuterons, ^{3}He and α-particles on various nuclei in the energy range 20-50 MeV per nucleon. The modifications of the experimental strategy enables the simultaneous measurement of the partial reaction cross section for 5 excluded forward cones, from which an extrapolation can be made to obtain the reaction cross section for the full solid angle.

The measurements were performed at the The Svedberg Laboratory, and the results

have been published elsewhere [4–6]. A measurement of 65 MeV protons has also been performed [7], and further proton measurements in the energy range 80-180 MeV have been performed at the iThemba Laboratory for Accelerator-Based Sciences.

---

[1] A.J. Koning, T. Fukahori and A. Hasegawa, NEA-REPORT NEA/WPEC-13, ECN-RX-98-014.

[2] R.F. Carlson, W.F. McGill, T.H. Short, J.M. Cameron, J.R. Richardson, W.T.H. van Oers, J.W. Verba, P. Doherty and D.J. Margaziotis, Nucl. Instr. and Meth. 123 (1975) 509.

[3] A. Auce, R.F. Carlson, A.J. Cox, A. Ingemarsson, R. Johansson, P.U. Renberg, O. Sundberg, G. Tibell and R. Zorro, Phys. Rev. C 50 (1994) 871.

[4] A. Auce, R.F. Carlson, A.J. Cox, A. Ingemarsson, R. Johansson, P.U. Renberg, O. Sundberg and G. Tibell, Phys. Rev. C 53 (1996) 2919.

[5] A. Ingemarsson, J. Nyberg, P.U. Renberg, O. Sundberg, R.F. Carlson, A.J. Cox, A. Auce, R. Johansson, G. Tibell, Dao T. Khoa and R.E. Warner, Nucl. Phys. A 653 (1999) 341.

[6] A. Ingemarsson, G.J. Arendse, A. Auce, R.F. Carlson, A.A. Cowley, A.J. Cox, S.V. Förtsch, R. Johansson, B.R. Karlson, M. Lantz, J. Peavy, J.A. Stander, G.F. Steyn and G. Tibell, Nucl. Phys. A 696 (2001) 3.

[7] A. Ingemarsson, J. Nyberg, P.U. Renberg, O. Sundberg, R.F. Carlson, A. Auce, R. Johansson, G. Tibell, B.C. Clark, L. Kurth Kerr and S. Hama, Nucl. Phys. A 653 (1999) 341.

[8] R.E. Warner, H. Thirumurthy, J. Woodroffe, F.D. Becchetti, J.A. Brown, B.S. Davids, A. Galonsky, J.J. Kolata, J.J. Kruse, M.Y. Lee, A. Nadasen, T.W. O'Donnell, D.A. Roberts, R.M. Ronningen, C. Samanta, P. Schwandt, J. von Schwarzenberg, M. Steiner, K. Subotich, J. Wang and J.A. Zimmerman, Nucl. Phys. A 635 (1998) 292.

[9] W. Mittig, J.M. Chouvel, Zhan Wen Long, L. Bianchi, A. Cunsolo, B. Fernandez, A. Foti, J. Gastebois, A. Gillibert, C. Gregoire, Y. Schutz and C. Stephan, Phys. Rev. Lett. 59 (1987) 1889.

[10] M.A. Farooq, I.E. Qureshi, M.I. Shahzad, S. Manzoor, H.A. Khan and M.S. Zafar, Rad. Meas. 33 (2001) 157, and references therein.

[11] H. Abele, U. Atzrott, A. Auce, C. Hillenmayer, A. Ingemarsson and G. Staudt, Phys. Rev. C 50, R10 (1994).

[12] V. F. E. Pucknell, http://nnsa.dl.ac.uk/MIDAS/.

[13] T. Sundqvist, J. Nyberg, TSL Progress Report 1996-1997, p. 21.

[14] P.U. Renberg, D.F Measday, M. Pepin, P. Schwaller, B. Favier and C. Richard-Serre, Nucl. Phys. A 183 (1972) 81.

[15] F. S. Dietrich, E. P. Hartouni, S. C. Johnson, G. J. Schmid, R. Soltz, W. P. Abfalterer, R. C. Haight, L. S. Waters, A. L. Hanson, R. W. Finlay and G. S. Blanpied, Jour. Nucl. Sci. and Technology, Supp. 2 (2002) 269.

[16] M. Lantz, M. N. Jacobs, A. Auce, R. F. Carlson, A. A. Cowley, S. F. Förtsch, G. C. Hillhouse, A. Ingemarsson, R. Johansson, K. J. Lawrie, M. J. Shachno, F. D. Smit, A. Stander, G. F. Steyn, G. Tibell and J. J. van Zyl, International Conference on Nuclear Data for Science and Technology, Santa Fe, 16 September - 1 October 2004.

[17] C. C. Chang, in Proceedings of the giant multipole resonance topical conference, Oak Ridge, 1979 p.191

[18] B. T. Murdoch, D. K. Hasell, A.M. Sourkes, W.T.H. van Oers and P.J.T. Verheijen, Phys. Rev. **C29** (1984) 2001.

[19] A. Houdayer, N. E. Davison, S. A. Elbakr, A. M. Sourkes, W. T. H. van Oers and A. D. Bacher, Phys. Rev. **18** (1978) 1985.